Cancer Cell
Article

gp130-Mediated Stat3 Activation in Enterocytes Regulates Cell Survival and Cell-Cycle Progression during Colitis-Associated Tumorigenesis

Julia Bollrath,[1,4] Toby J. Phesse,[2,4] Vivian A. von Burstin,[1] Tracy Putoczki,[2] Moritz Bennecke,[1] Trudie Bateman,[2,5] Tim Nebelsiek,[1] Therese Lundgren-May,[2] Özge Canli,[1] Sarah Schwitalla,[1] Vance Matthews,[2,6] Roland M. Schmid,[1] Thomas Kirchner,[3] Melek C. Arkan,[1] Matthias Ernst,[2,*] and Florian R. Greten[1,*]

[1]2nd Department of Medicine, Klinikum rechts der Isar, Technical University Munich, 81675 Munich, Germany
[2]Ludwig Institute for Cancer Research Ltd., Royal Melbourne Hospital, Parkville, VIC 3050, Australia
[3]Institute of Pathology, Ludwig-Maximilians-Universität, 80337 Munich, Germany
[4]These authors contributed equally to this work
[5]Present address: Arana Therapeutics Limited, 343 Royal Parade, Parkville, VIC 3052, Australia
[6]Present address: Baker IDI Heart and Diabetes Institute, St Kilda Road Central, Prahran, VIC 8008, Australia
*Correspondence: matthias.ernst@ludwig.edu.au (M.E.), florian.greten@lrz.tum.de (F.R.G.)
DOI 10.1016/j.ccr.2009.01.002

SUMMARY

Although gastrointestinal cancers are frequently associated with chronic inflammation, the underlying molecular links have not been comprehensively deciphered. Using loss- and gain-of-function mice in a colitis-associated cancer model, we establish here a link comprising the gp130/Stat3 transcription factor signaling axis. Mutagen-induced tumor growth and multiplicity are reduced following intestinal epithelial cell (IEC)-specific Stat3 ablation, while its hyperactivation promotes tumor incidence and growth. Conversely, IEC-specific Stat3 deficiency enhances susceptibility to chemically induced epithelial damage and subsequent mucosal inflammation, while excessive Stat3 activation confers resistance to colitis. Stat3 has the capacity to mediate IL-6- and IL-11-dependent IEC survival and to promote proliferation through G1 and G2/M cell-cycle progression as the common tumor cell-autonomous mechanism that bridges chronic inflammation to tumor promotion.

INTRODUCTION

Persistent and aberrant activation of various members of the signal transducer and activator of transcription (STAT) family is a recurrent and unifying molecular feature of many human malignancies of hematological and epithelial origin (Levy and Darnell, 2002; Yu and Jove, 2004). Among the seven STAT proteins, hyperactivation of STAT3 has been shown to promote tumor growth directly by tumor-autonomous mechanisms as well as indirectly by regulating the antitumor response of the tumor-associated stroma and the immune system. Thus, STAT3 plays a pivotal role in the regulation of transcriptional programs that are essential prerequisites for carcinogenesis (Hanahan and Weinberg, 2000), including those regulating cell survival, proliferation, angiogenesis, and tumor-induced immunosuppressive functions (Yu et al., 2007). Meanwhile, many of the major signal transduction pathways activated in cancer and initiated by the receptor tyrosine kinases for epidermal, platelet-derived, and vascular endothelial growth factors, by cytokines of the interleukin-6 (IL-6) and IL-10 families, or by non-receptor tyrosine kinases converge on STAT3. Indeed, aberrant activation of STAT3 in human cancers is invariably associated with the presence of constitutive activating mutations in upstream (receptor) tyrosine kinases or tumor-associated oversupply of the aforementioned ligands, while such mutations in the *STAT3* gene have not been identified. These observations

SIGNIFICANCE

Aberrant Stat3 activation is a recurrent finding in many tumors, but the mechanism (or mechanisms) by which Stat3 links inflammation to cancer remains elusive. Using genetically modified mouse strains that harbor mutations in the Stat3 signaling cascade, we here identify in an inflammation-associated colon cancer model a dual role for mucosal Stat3 in mediating an anti-inflammatory cytoprotective effect as well as in enhancing tumor growth. Thus, upon stimulation by IL-6 family cytokines, which are produced by inflammatory and other tumor-associated cells, Stat3 acts as a unifying cancer cell-autonomous transcription factor node that simultaneously enables survival of mutagenized cells and subsequent tumor promotion in situ.

are consistent with the tyrosine phosphorylation requirement of latent cytoplasmic STAT3 to form dimers that are able to bind to DNA and to regulate transcription. Likewise, epigenetic impairment mutations in genes encoding negative regulators of STAT3 signaling, including the tyrosine phosphatase PTPRT and suppressor of cytokine signaling 3 (SOCS3), result in persistent STAT3 activation and associated tumorigenesis (He et al., 2003; Zhang et al., 2007).

Gene deletion studies in mice have identified a nonredundant function for Stat3 in transducing signals from the common IL-6 cytokine family receptor β subunit gp130 (Heinrich et al., 2003). In order for signaling to be initiated, gp130 requires either homodimerization, which is induced upon binding of IL-6 or IL-11 to their respective receptor α subunits, or heterodimerization with structurally related receptor β subunits in response to the remaining ligands that comprise the IL-6 cytokine family (Heinrich et al., 2003). In either case, β subunit dimerization triggers activation of associated Janus kinases and subsequent phosphorylation of cytoplasmic tyrosine (Y) residues, whereby the four membrane-distal tyrosines engage Stat3 and to a lesser extent Stat1. Meanwhile, ligand-dependent gp130 phosphorylation of the most membrane-proximal residue Y757 (Y759 in human gp130) results in engagement of the tyrosine phosphatase Shp2 and activation of the downstream Ras/Erk and PI3K/Akt signaling cascades, as well as providing the binding site for the regulatory protein Socs3, which serves to limit gp130 signaling.

A causal link between inflammation and cancer is well accepted (Karin and Greten, 2005; Mantovani et al., 2008), and several recent studies in genetically modified mice have helped to dissect and characterize some of the underlying molecular events. One major regulatory pathway linking inflammation and cancer comprises IKKβ-dependent activation of NF-κB (Karin and Greten, 2005). Elevated NF-κB activity in premalignant epithelial cells suppresses apoptosis, thereby promoting their survival and subsequent capacity to form tumors. Meanwhile, engagement of the same pathway in tumor-associated inflammatory cells initiates transcription of proinflammatory cytokines, which in turn stimulate the proliferation of tumor and stromal cells to further fuel tumor growth (Karin and Greten, 2005). One of the NF-κB-dependent inflammatory growth factors thought to be essential for inflammation-associated carcinogenesis is IL-6 (Naugler and Karin, 2008). Indeed, in a colitis-associated cancer (CAC) model wherein chronic inflammation triggered through administration of the luminal toxin dextran sodium sulfate (DSS) reveals the mutagenic effect of prior exposure to the colonotropic mutagen azoxymethane (AOM), we recently proposed that myeloid-specific deletion of IKKβ suppresses tumor incidence and size at least in part through reduced myeloid-specific *Il6* transcription (Greten et al., 2004). T lymphocytes furthermore regulate tumor growth in the CAC model via a TGF-β-dependent mechanism that limits IL-6 *trans*-signaling, because its inhibition by administration of either neutralizing IL-6 receptor α chain antibodies or soluble gp130-Fc suppresses enterocyte-specific Stat3 activation and proliferation and culminates in reduced tumor incidence (Becker et al., 2004). Recent circumstantial evidence has further promoted the concept that the IL-6/gp130/Stat3 signaling axis may also provide an autocrine and paracrine amplification loop in lung adenocarcinoma (Gao et al., 2007), multiple myeloma (Catlett-Falcone et al., 1999), and Ras-transformed cancer cells (Ancrile et al., 2007). Thus, Stat3 is likely to serve as the signaling node that integrates tumor cell-autonomous signals with tumorigenic cues indirectly provided through the immune system.

Here we genetically manipulated Stat3 expression and activation in the intestinal epithelium using various gain-of-function and loss-of-function mouse models to define and dissect the causal role played by Stat3 during CAC-induced colonic tumorigenesis. We define a function for Stat3 in the intestinal epithelium, where it mediates resistance to DSS-induced epithelial damage and promotes tumorigenesis. Therefore, the capacity of Stat3 to suppress apoptosis and stimulate proliferation not only facilitates colitis-associated wound healing but at the same time also promotes mutagen-induced tumor growth. These observations demonstrate that, in addition to IKKβ-dependent NF-κB activation, Stat3 may comprise a central node and checkpoint during inflammation-associated carcinogenesis and is therefore likely to represent a promising target for therapeutic intervention.

RESULTS

Intestinal Stat3 Activity Modulates Colitis-Associated Tumorigenesis

To directly examine the effect of Stat3 expression in colonic epithelium during the process of CAC, we generated compound mutant mice that lacked Stat3 specifically in all epithelial cell lineages of the intestine. These mice carried a homozygous mutation encompassing a loxP-flanked exon 21 of the *Stat3* gene ($Stat3^{flox}$) (Takeda et al., 1998) and simultaneously expressed Cre recombinase under the control of the intestine-specific *villin* gene promoter (*villin*-Cre) (Madison et al., 2002). Since villin is ubiquitously expressed throughout the epithelial layer of the intestine, including the presumed stem cell compartment, we confirmed the absence of full-length Stat3 protein in the resulting homozygous $Stat3^{\Delta IEC}$ mice by immunoblot analysis of isolated intestinal epithelial cells (IECs) from their small and large intestines, respectively (see Figure S1 available online). IEC-specific Stat3 deficiency had no effect on the development and function of the intestine in adult mice, and the baseline rate of proliferation and apoptotic index were indistinguishable under steady-state conditions between unchallenged $Stat3^{flox}$ and $Stat3^{\Delta IEC}$ mice (Figure S1). Furthermore, $Stat3^{\Delta IEC}$ mice were healthy and fertile and did not display any overt phenotype when routinely bred for up to 4 months of age.

Next, we exposed $Stat3^{\Delta IEC}$ mice to the CAC challenge and found that they were almost completely protected from the development of AOM-induced tubular adenomas (Figure 1A), while 100% of Stat3-proficient $Stat3^{flox}$ mice (8 of 8) developed adenomatous lesions in the distal colon (Figures 1A and 1C). Furthermore, the few polypoid lesions protruding into the lumen that developed in the small proportion of $Stat3^{\Delta IEC}$ mice (2 of 8) (Figure 1D) were markedly reduced in size (Figure 1B). To explore a possible dose-response relationship between Stat3 activation and CAC-dependent tumorigenesis, we took advantage of the $gp130^{Y757F}$ mouse model, in which IL-6 and IL-11 trigger global Stat3 hyperactivation, including in the colonic epithelium (Figure S2) (Jenkins et al., 2005; Tebbutt et al., 2002). As opposed to our findings in $Stat3^{\Delta IEC}$ mice, we observed

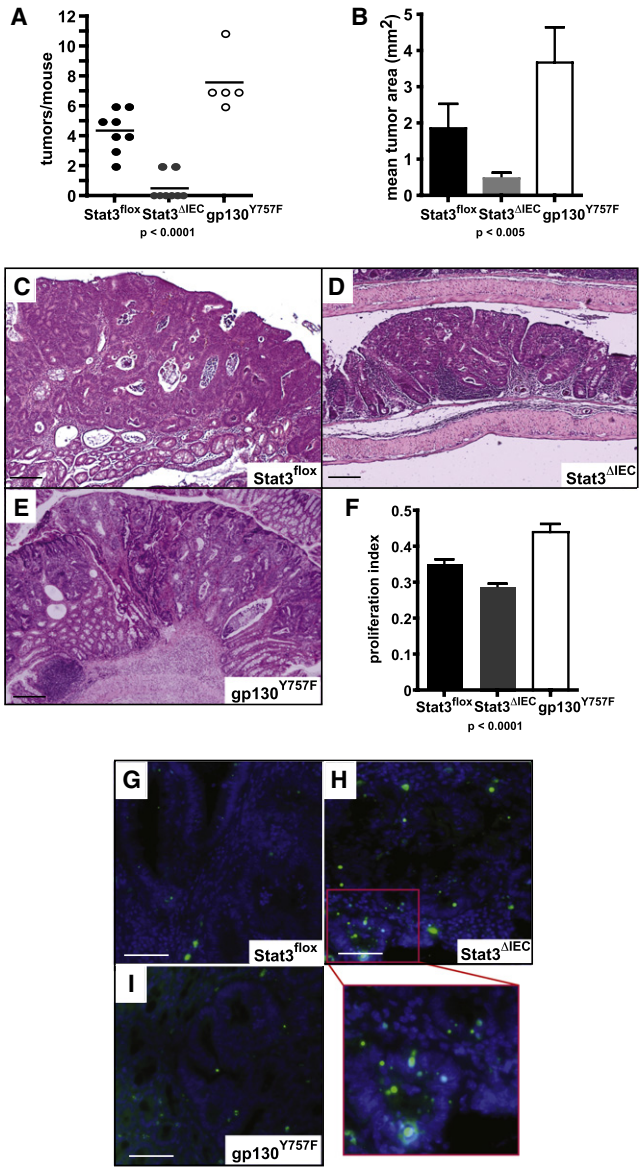

Figure 1. Stat3 Is Essential for Colitis-Associated Tumor Development

(A and B) Tumor incidence (A) and mean tumor size (B) in *Stat3*^{flox}, *Stat3*$^{\Delta IEC}$, and *gp130*^{Y757F} mice after completion of the colitis-associated cancer (CAC) challenge at day 84.

(C–E) Hematoxylin and eosin (H&E)-stained sections of colons from mice at the end of the CAC challenge (day 84) showing representative adenomatous polyps protruding into the colonic lumen in *Stat3*^{flox} mice (C), *Stat3*$^{\Delta IEC}$ mice (D), and *gp130*^{Y757F} mice (E). Scale bars = 200 μm.

(F) BrdU proliferation index of epithelial cells in polyps protruding into the lumen of *Stat3*^{flox}, *Stat3*$^{\Delta IEC}$, and *gp130*^{Y757F} mice.

(G–I) Assessment of apoptosis by TUNEL staining of tumors from *Stat3*^{flox} (G), *Stat3*$^{\Delta IEC}$ (H), and *gp130*^{Y757F} mice (I) on day 84 of the CAC challenge. Scale bars = 100 μm. A magnified view of the boxed area from the *Stat3*$^{\Delta IEC}$ mouse in (H) confirms that TUNEL-positive signals originate primarily from epithelial cells. Note that CAC-dependent tumor incidence in *gp130*^{Y757F} animals was compared to that in wild-type littermate controls, which showed tumor incidence and size comparable to *Stat3*^{flox} mice and were therefore omitted from the graphs. Data are mean ± SEM. Differences between groups were analyzed by one-way ANOVA.

increased multiplicity of frequency and size of AOM + DSS-induced tumors in *gp130*^{Y757F} mice (Figures 1A, 1B, and 1E) when compared to wild-type mice. To assess the consequence of manipulating Stat3 expression or activation on tumor cell proliferation, we determined BrdU incorporation in tumor epithelia. In agreement with a profound effect on tumor size, we observed a significant reduction of the BrdU proliferation index in *Stat3*$^{\Delta IEC}$ mice, which was elevated by 25% in *gp130*^{Y757F} mice when compared to *Stat3*^{flox} mice (Figure 1F). By contrast, TUNEL analysis revealed a reciprocal increase in the apoptotic response of the colonic mucosa in *Stat3*$^{\Delta IEC}$ mice when compared to *Stat3*^{flox} and *gp130*^{Y757F} mice (Figures 1G–1I). Collectively, the results obtained with the direct Stat3 loss-of-function (*Stat3*$^{\Delta IEC}$) model and the indirect gp130-dependent Stat3 gain-of-function (*gp130*^{Y757F}) model implicate a dose-response relationship between epithelial Stat3 activation and colonic tumor incidence as well as tumor growth in the CAC model.

Interestingly, we found that despite the smaller number and size of tumors in *Stat3*$^{\Delta IEC}$ mice, these lesions were consistently associated with more severe colonic mucosal inflammation and greater tissue damage than observed in *Stat3*^{flox} mice (Figures 2B–2F). However, it remained unclear whether the exaggerated inflammatory response in *Stat3*$^{\Delta IEC}$ mice was compounded by the initial mutagenic challenge. Therefore, we exposed *Stat3*$^{\Delta IEC}$ mice to three cycles of DSS without the initial AOM challenge and found that this treatment also resulted in extensive ulceration and epithelial damage scores that were significantly higher in *Stat3*$^{\Delta IEC}$ compared to *Stat3*^{flox} control mice (Figure S3). Collectively, these observations suggest a strong protective role for Stat3 in IECs during chronic colitis, and they argue against the possibility that tumor development is suppressed in *Stat3*$^{\Delta IEC}$ mice because of less pronounced mucosal inflammation.

AOM induces missense mutations in exon 3 of *Catnb* that lead to stabilization and nuclear translocation of β-catenin, thereby activating the Wnt/β-catenin pathway (Greten et al., 2004). Activation of this signaling pathway triggers formation of colonic flat low-grade intraepithelial neoplasias, which then further progress into tubular adenomas in wild-type and *Stat3*^{flox} mice. Instead of developing these advanced tubular tumors, CAC-challenged *Stat3*$^{\Delta IEC}$ mice displayed multifocal flat low-grade intraepithelial neoplasias in active colitis (Figure 2G and 2H). To confirm that the latter lesions indeed genetically represented tumor precursors, we applied laser capture microdissection (LCM) to isolate DNA from epithelial cells from intraepithelial neoplastic lesions as well as from the few CAC-induced advanced tubular adenomas from *Stat3*$^{\Delta IEC}$ mice. We consistently identified activating mutations in exon 3 of *Catnb* in all lesions of *Stat3*$^{\Delta IEC}$ mice examined (data not shown) and also confirmed deletion of exon 21 of *Stat3* (data not shown). Furthermore, similar mutations in *Catnb* were found in DNA isolated by LCM from *Stat3*^{flox} tubular adenomas, while the majority of tubular adenomas isolated from *gp130*^{Y757F} mice showed nuclear localization of activated β-catenin (Figure S4), consistent with AOM-induced activating *Catnb* mutations. Collectively, we conclude from these observations that epithelial depletion of Stat3 blocks early tumor development and that the extent of Stat3 activation modifies canonical Wnt signaling-initiated tumorigenesis.

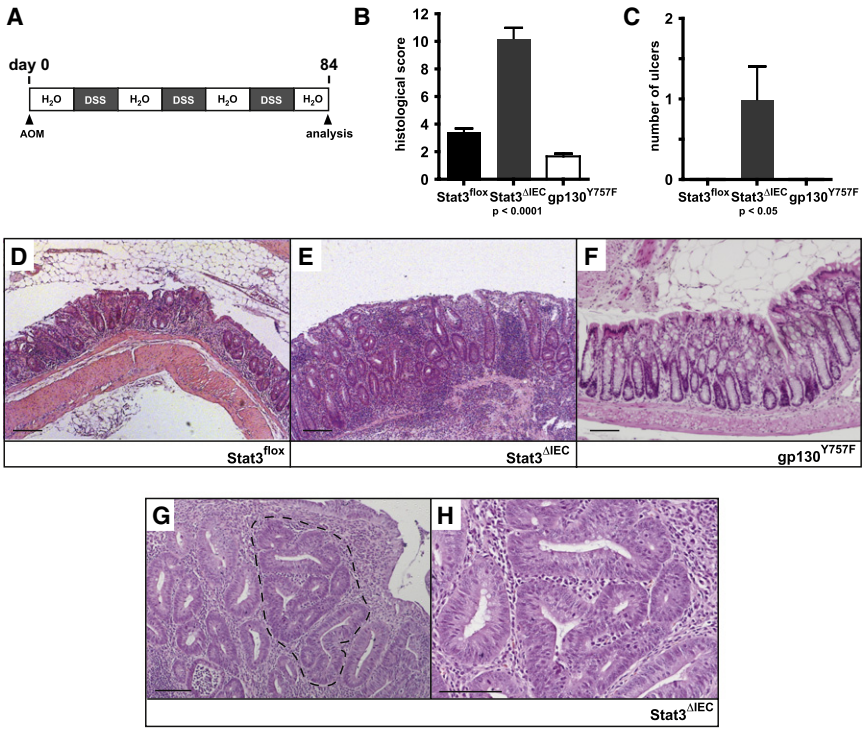

Figure 2. Increased Epithelial Damage and Infiltration of Inflammatory Cells in *Stat3*$^{\Delta IEC}$ Mice after Completion of the CAC Challenge

(A) Schematic representation of the CAC model.

(B and C) Histological damage (B) and number of ulcers (C) in *Stat3*^{flox}, *Stat3*$^{\Delta IEC}$, and *gp130*^{Y757F} mice analyzed on day 84 of the CAC model. Data are mean ± SEM. n = 8.

(D–F) Representative H&E-stained sections demonstrating varying degrees of inflammation in mice of the indicated genotypes. Scale bars = 200 μm.

(G and H) Representative H&E-stained section of multifocal flat low-grade intraepithelial neoplasia (indicated by dashed line) frequently found in *Stat3*$^{\Delta IEC}$ mice at the end of the CAC challenge (G) as well as a larger magnification of this tumor precursor (H). Scale bars = 100 μm.

Stat3 Protects Enterocytes from Apoptosis during Early Tumor Promotion

We have shown previously that ablation of IKKβ in either enterocytes or myeloid cells affects apoptosis and proliferation during the early stages of tumor promotion in the CAC model, thereby reducing tumor incidence and size, respectively (Greten et al., 2004). We thus focused our analysis on these time points to elucidate the molecular mechanisms by which Stat3 confers its tumorigenic properties. To examine whether IEC-specific deletion of Stat3 renders enterocytes more susceptible to apoptosis at the beginning of the CAC protocol, we injected *Stat3*^{flox} and *Stat3*$^{\Delta IEC}$ mice with AOM and sacrificed them 3 days after initiation of DSS treatment, which corresponds to day 8 of the CAC regimen (Figure 3A). Immunohistochemical analysis revealed enterocyte-specific nuclear localization of the tyrosine-phosphorylated (activated) form of Stat3 (p-Stat3) in *Stat3*^{flox} mice (Figure 3B), and this signal was completely absent from IECs in colons of *Stat3*$^{\Delta IEC}$ mice (Figure 3C), which was further confirmed by immunoblot analysis of purified epithelial cells (Figure 3H). The lack of Stat3 activation in *Stat3*$^{\Delta IEC}$ mice coincided with the presence of extended areas of epithelial apoptosis in the mucosa as visualized by immunohistochemical staining for active caspase-3 (Figures 3D and 3E) and by TUNEL (Figures 3F and 3G). Biochemical analysis confirmed pronounced activation (cleavage) of caspase-9 and thus an increased apoptotic response in isolated Stat3-deficient colonocytes (Figure 3H) when compared to IECs from *Stat3*^{flox} mice. Meanwhile, in Stat3-proficient *Stat3*^{flox} mice, we observed induction of the anti-apoptotic proteins Bcl-X_L and survivin, as well as upregulation of the ATP-dependent chaperone protein Hsp70. In contrast, colonocytes derived from challenged *Stat3*$^{\Delta IEC}$ mice failed to reveal upregulation of these proteins, consistent with findings by others that the *bcl-x*, *survivin*, and *Hspa1a* (encoding Hsp70) genes are transcriptionally induced by Stat3 (Yu and Jove, 2004). Interestingly, we found constitutive expression of Bcl-2 and Stat3-independent induction of Mcl-1 (Figure 3H), despite the fact that these two anti-apoptotic proteins are also encoded by presumed Stat3 target genes (Yu and Jove, 2004). Similarly, we observed constitutive expression of the proapoptotic proteins Bax and Bak, while the induction of Fas/CD95 also occurred independently of Stat3. Collectively, these results suggest that impaired induction of Bcl-X_L, survivin, and Hsp70 protein expression, rather than differential regulation of Bcl-2, Mcl-1, Bak, and Bax, may account for the increased rate of apoptosis observed in AOM + DSS-challenged *Stat3*$^{\Delta IEC}$ mice.

Stat3 Stimulates Regeneration and Proliferation during Colitis

DSS-induced apoptosis leads to an epithelial barrier defect and translocation of bacterial commensals, which initiate an inflammatory cascade. Once DSS administration is suspended, colonic epithelium can regenerate and inflammation resolves. This mucosal regeneration stage represents a wound-healing reaction during which hyperproliferation of epithelial cells is stimulated by proinflammatory cytokines and growth factors that are secreted by recruited inflammatory cells. Thus, we hypothesized that the increased initial apoptosis in *Stat3*$^{\Delta IEC}$ mice should indirectly induce a more severe form of acute colitis. Indeed, when we monitored body weights during the first cycle of DSS-induced acute colitis after AOM administration, *Stat3*$^{\Delta IEC}$ mice lost significantly more weight than *Stat3*^{flox} mice (Figure 4A). More importantly, *Stat3*^{flox} mice rapidly regained normal body weight a few days after removal of DSS from the drinking water, while *Stat3*$^{\Delta IEC}$ mice exhibited a delayed recovery. This was further supported by histopathological analysis of mice at day 15 of the CAC regimen, 5 days after termination of DSS administration. We found that colons of *Stat3*$^{\Delta IEC}$ mice exhibited widespread damage to the colonic mucosa, with extensive epithelial denudation and larger numbers of ulcerations compared to the partially preserved epithelial structures observed in *Stat3*^{flox}

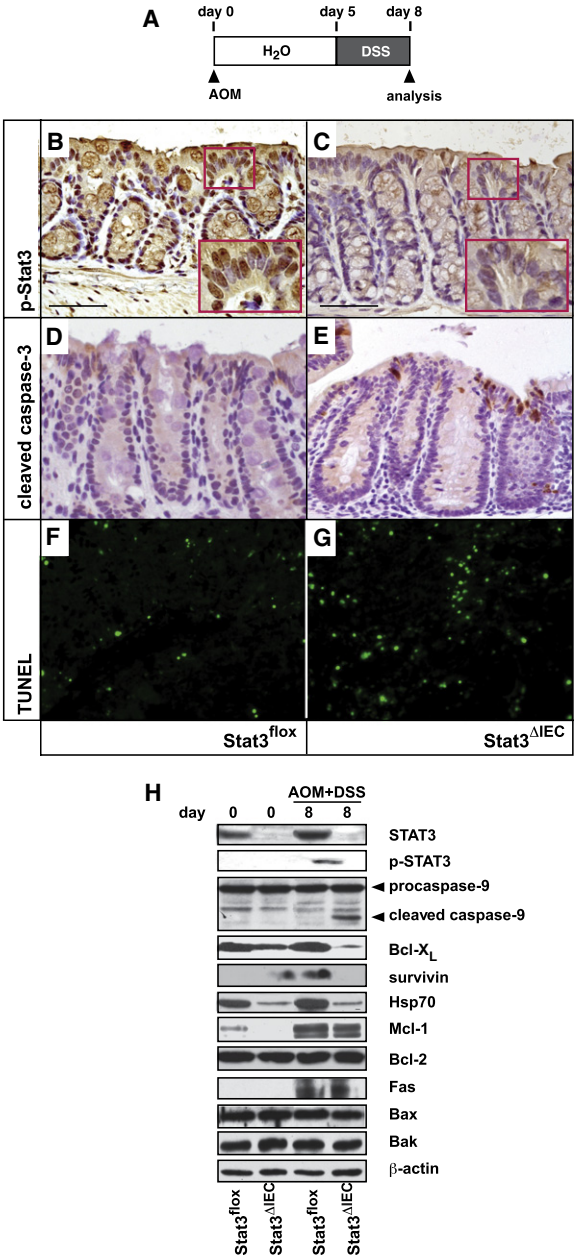

Figure 3. Loss of Stat3 in Intestinal Epithelial Cells Sensitizes Enterocytes to Apoptosis Early after AOM and DSS Administration

(A) Schematic representation of the initial steps of the CAC challenge that results in maximal apoptotic response on day 8 of the CAC regimen.

(B–G) Immunohistochemical analysis of phospho-Stat3 (B and C), cleaved caspase-3 (D and E), and TUNEL staining (F and G) of colons from *Stat3*^{flox} mice (B, D, and F) and *Stat3*$^{\Delta IEC}$ mice (C, E, and G). Insets in (B) and (C) demonstrate nuclear localization of phospho-Stat3 in *Stat3*^{flox} mice (B) that is absent from enterocytes in *Stat3*$^{\Delta IEC}$ mice (C). Scale bars = 100 μm.

(H) Immunoblot analysis for the indicated proteins in lysates prepared from isolated enterocytes from *Stat3*^{flox} and *Stat3*$^{\Delta IEC}$ mice at day 8 of the CAC challenge.

mice (Figures 4B–4E), where we confirmed Stat3 activation in colonic enterocytes (Figures 4F and 4G). Meanwhile, the extensive hyperinflammatory response in *Stat3*$^{\Delta IEC}$ mice associated with the increased epithelial damage was accompanied by elevated expression of mRNAs encoding IL-1β, IL-6, IL-11, Cox-2, ICAM-1, and IL-10 in the colonic mucosa of these mice, whereas no differences were observed in TNFα and IFN-γ expression (Figure 4I). However, despite a more profound inflammatory response and the associated increase in growth-stimulating signals in *Stat3*$^{\Delta IEC}$ mice, BrdU incorporation studies revealed impaired proliferation of their colonic enterocytes as compared to colonic crypts of *Stat3*^{flox} mice (Figure 4J).

The increased inflammatory reaction and wound-healing defect observed in *Stat3*$^{\Delta IEC}$ mice was reminiscent of our previous findings in *gp130*$^{\Delta STAT}$ mice (Tebbutt et al., 2002) and therefore strongly suggested that the lost capacity of epithelial cells to activate Stat3 in response to IL-6 family cytokines was primarily responsible for DSS-induced mucosal damage. This conclusion is supported by the converse finding that *gp130*^{Y757F} mutant mice, which carry a knockin mutation to confer ligand-dependent Stat3 and Stat1 hyperactivation, remain largely protected against colonic epithelial injury (Tebbutt et al., 2002). In order to genetically confirm that this effect is selectively conferred by Stat3 rather than Stat1 hyperactivation, we genetically reduced the global pool of either Stat3 or Stat1 available for activation in *gp130*^{Y757F} mice. Indeed, the protective effect observed in *gp130*^{Y757F} mice was partially reverted in the corresponding *gp130*^{Y757F}/*Stat3*$^{+/-}$ mice but was retained in *gp130*^{Y757F}/*Stat1*$^{+/-}$ mice (Figure S5). Having established that the clinical protection against DSS-induced colitis of *gp130*^{Y757F} mice is largely dependent on Stat3 hyperactivation, we examined whether *gp130*^{Y757F} mice would also display a phenotype reciprocal to that of *Stat3*$^{\Delta IEC}$ mice with respect to the proliferative mucosal wound-healing reaction. In line with the decreased mucosal susceptibility of *gp130*^{Y757F} mice to DSS, we found that BrdU incorporation after DSS challenge was significantly higher in IECs of *gp130*^{Y757F} mutant mice than in IECs of wild-type mice (Figures 5A–5C).

Since impaired expression of Stat3 in myeloid cells results in enhanced susceptibility to colitis (Takeda et al., 1999) and since *gp130*^{Y757F} mice exhibit systemic gp130-dependent Stat3 hyperactivation, we next wished to determine whether the protective effect observed in *gp130*^{Y757F} mutants is independent of the anti-inflammatory response elicited in macrophages of these mice (El Kasmi et al., 2006). We therefore performed reciprocal bone-marrow reconstitution experiments in *gp130*^{Y757F} and wild-type mice 2 months prior to DSS challenge and observed that the presence of mutant hematopoietic cells did not reduce susceptibility of wild-type hosts to the DSS challenge (Figure S6). On the other hand, *gp130*^{Y757F} mutant hosts remained more resistant to DSS than wild-type hosts, irrespective of the genotypes of their hematopoietic cells. These clinical observations matched differential BrdU incorporation results, which were elevated in the resistant *gp130*^{Y757F} mutant hosts (Figure 5C). Collectively, these results argue in favor of an IEC-autonomous mechanism by which Stat3-dependent hyperproliferation mediates the protective effect against DSS-induced colitis. This conclusion is also supported by our observation that IEC-specific overexpression of a mutant form of constitutively active Lgp130 (Stuhlmann-Laeisz et al., 2006) confers resistance to DSS-induced colitis in transgenic mice (T.P. and M.E., unpublished data).

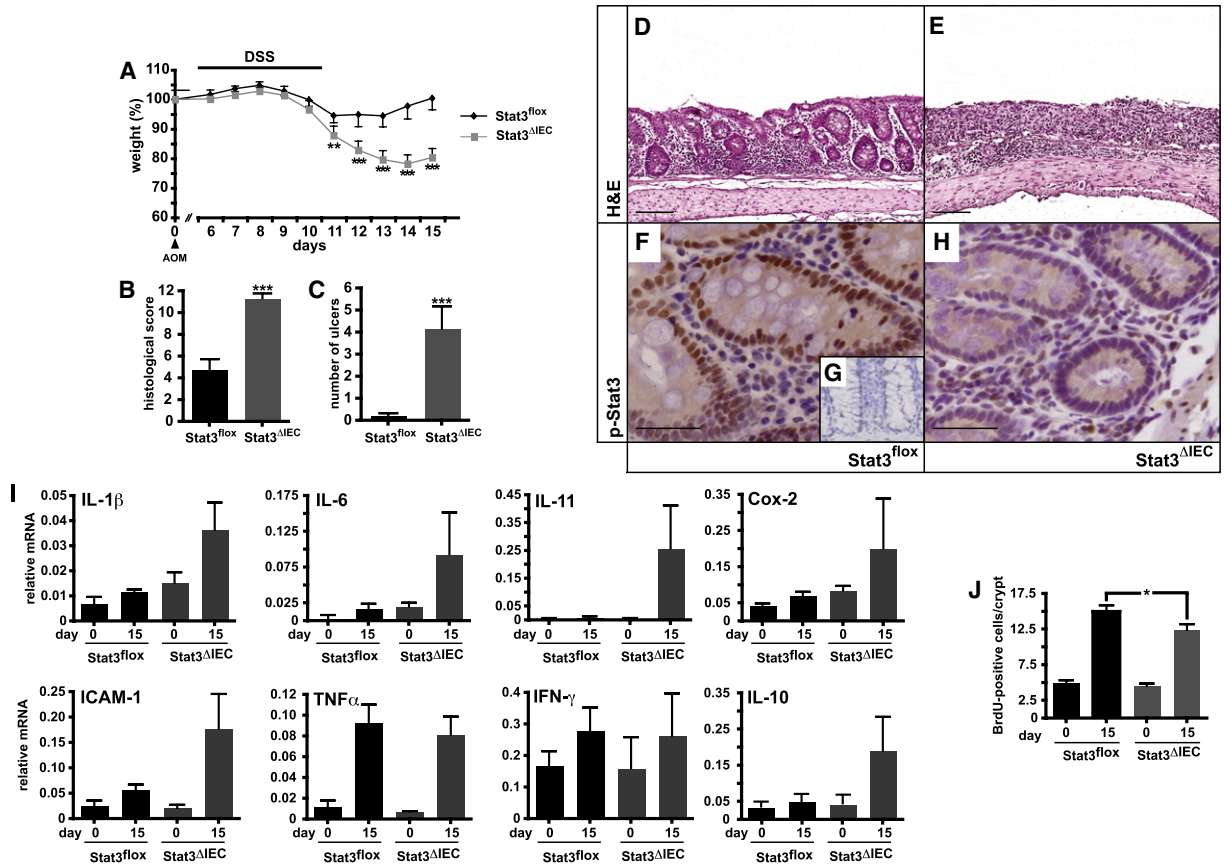

Figure 4. *Stat3*$^{\Delta IEC}$ Mice Develop More Severe Acute Ulcerative Colitis during the CAC Regimen and Show Impaired Mucosal Wound Healing

(A) Changes in body weight of *Stat3*^{flox} and *Stat3*$^{\Delta IEC}$ mice during the first cycle of acute DSS-induced colitis. Five days after AOM treatment, mice were administered 3.5% DSS in the drinking water for 5 days, followed by a 5 day recovery phase on normal drinking water. All mice were sacrificed and analyzed on day 15 of the CAC regimen. Data are mean ± SEM. $n \geq 7$; $^{**}p < 0.01$, $^{***}p < 0.001$ by t test.

(B and C) Histological damage (B) and number of ulcers (C) in *Stat3*^{flox} and *Stat3*$^{\Delta IEC}$ mice analyzed at day 15 of the CAC model. Data are mean ± SEM. $n \geq 7$; $^{***}p < 0.001$ by t test.

(D–H) Representative H&E-stained sections (D and E) and immunohistochemical analysis of phospho-Stat3 (F–H) of colons from *Stat3*^{flox} mice (D and F) and *Stat3*$^{\Delta IEC}$ mice (E and H) at day 15 of the CAC challenge or in an unchallenged *Stat3*^{flox} mouse (G). Scale bars = 100 μm.

(I) Relative expression levels of cytokine mRNAs isolated from whole colonic mucosa of *Stat3*^{flox} and *Stat3*$^{\Delta IEC}$ mice at day 15 of the CAC model and analyzed by real-time PCR. Data are mean ± SEM. $n \geq 3$.

(J) BrdU proliferation index in colonic enterocytes of *Stat3*^{flox} and *Stat3*$^{\Delta IEC}$ mice before and at day 15 of the CAC challenge. Data are mean ± SEM. $n \geq 7$; $^{*}p < 0.05$ by t test.

Previously we showed that IL-11 signaling, rather than IL-6 signaling, promotes tumorigenesis in a model of inflammation-associated gastric cancer (Ernst et al., 2008), while IL-6 has been proposed to play this role in the CAC model (Becker et al., 2004; see also the accompanying paper by Grivennikov et al. [2009] in this issue of *Cancer Cell*). We therefore examined genetically which of these cytokines triggers the colitis-protective proliferative phenotype in *gp130*^{Y757F} mice. Whereas double-mutant *gp130*^{Y757F}/*Il6*$^{-/-}$ and *gp130*^{Y757F}/*Il11ra*$^{-/-}$ mice exhibited a hyperproliferative phenotype similar to *gp130*^{Y757F} mice (Figure 5D), only the corresponding triple-compound *gp130*^{Y757F}/*Il11ra*$^{-/-}$/*Il6*$^{-/-}$ mutant mice, which simultaneously lack IL-6 and IL-11 signaling, showed a significant reduction in BrdU-positive IECs after DSS challenge (Figure 5D). These results suggest redundant activity for the latter two cytokines in eliciting a gp130/Stat3-dependent proliferative mucosal response, which is therefore likely to also promote inflammation-associated tumor progression in the colon.

Hyperproliferation in *gp130*^{Y757F} Mice Is Associated with Cell-Cycle Alterations during G1 and G2/M Phase

We next aimed to identify genes that are induced at the height of the Stat3-mediated proliferative response. Therefore, we isolated RNA from IECs of *gp130*^{Y757F} and wild-type mice at day 12 of the CAC model (Figure 6A) and performed quantitative PCR analysis for cell-cycle genes encoding the late G1 to G1/S phase proteins cyclin D1, cyclin D2, cyclin E, and c-Myc; the G2/M phase proteins cdc2 and cyclin B1; and the cyclin-dependent kinase (Cdk) inhibitor p21^{cip}. Although basal expression of cyclins D2 and E was comparable between wild-type and *gp130*^{Y757F} mice, we found that AOM + DSS treatment induced expression of cyclin D1, c-Myc, cyclin B1, and cdc2 that was

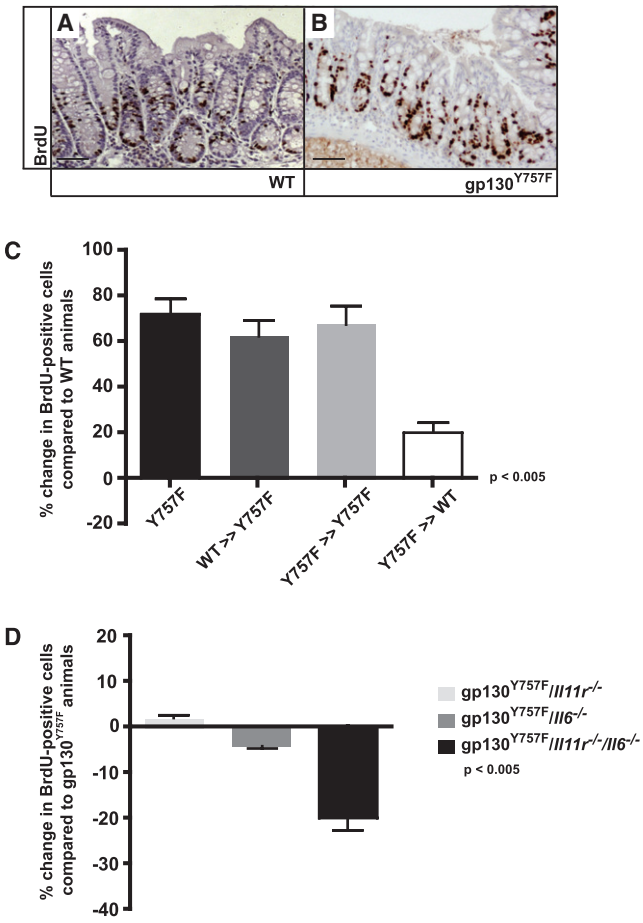

Figure 5. IL-6 and IL-11 Induce Intestinal Epithelial Cell Hyperproliferation in *gp130*^{Y757F} Mice during the Healing Phase of Acute Colitis

(A and B) BrdU incorporation in colonic crypts of wild-type (A) and *gp130*^{Y757F} mice (B) after one cycle of DSS-induced colitis, 1 day after termination of DSS administration. Scale bars = 100 μm.

(C) Relative change in BrdU incorporation in colonic crypts of *gp130*^{Y757F} mice or respective bone marrow-transplanted mice compared to wild-type mice after one cycle of DSS-induced colitis (WT > > Y757F indicates wild-type bone marrow transplanted into *gp130*^{Y757F} recipient mice).

(D) Relative change in BrdU incorporation in colonic crypts of *gp130*^{Y757F}/*Il11ra*$^{-/-}$, *gp130*^{Y757F}/*Il6*$^{-/-}$, and *gp130*^{Y757F}/*Il11ra*$^{-/-}$/*Il6*$^{-/-}$ compound mutants compared to single-mutant *gp130*^{Y757F} mice after one cycle of DSS-induced colitis.

BrdU-positive cells were only determined in well-oriented crypts. Data are averages of 15 crypts/mouse, n ≥ 5. Data are mean ± SEM. Differences between genotypes were analyzed by one-way ANOVA.

more pronounced in *gp130*^{Y757F} mice (Figure 6B) than in wild-type mice. This suggested a stimulatory effect of Stat3 on G1 and G2/M transition of the cell cycle, and this observation was consistent with more profound downregulation of the Cdk inhibitor p21^{cip} in IECs from *gp130*^{Y757F} mice. To confirm that these alterations conferred increased cyclin-dependent kinase activity, we performed immunocomplex kinase assays for cdk4/cyclin D and cdc2/cyclin B using GST-Rb and histone H1 as substrates, respectively. Although we observed elevated activity for both kinase complexes in IECs of AOM + DSS-treated wild-type mice, this effect was stronger in IECs prepared from challenged *gp130*^{Y757F} mice (Figure 6C). In contrast, the activity of these kinase complexes as well as the expression of cyclin D1 and c-Myc was blunted in IECs from AOM + DSS-treated *Stat3*$^{\Delta IEC}$ mice, while p21^{cip} expression was elevated (Figures 6C and 6D), further supporting our findings that these effects are indeed dependent on the extent of Stat3 activation. Meanwhile, we found strong nuclear expression of cyclin B1 in the epithelial cell components of the AOM-induced tumors in wild-type and *gp130*^{Y757F} mice, which was almost completely absent from the polyp precursors observed in *Stat3*$^{\Delta IEC}$ mice (Figures 7A and 7B; data not shown). Conversely, intraepithelial neoplastic lesions in *Stat3*$^{\Delta IEC}$ mice showed a significantly higher number of IEC nuclei that stained positive for the M phase cell-cycle marker phosphohistone H3 (Figures 7C and 7D). Collectively, these findings strongly suggest a mitotic arrest in Stat3-deficient, AOM-mutagenized IECs that is likely to provide a molecular explanation for the pronounced growth arrest of polyp precursors in *Stat3*$^{\Delta IEC}$ mice.

Finally, we wished to establish whether the antiapoptotic response observed in IECs of Stat3-proficient mice during early phases of the DSS challenge (see Figure 3H) persisted through the stages of maximal wound healing observed 2 days after the DSS challenge, corresponding to day 12 of the CAC regimen (Figure 6A). Indeed, we observed that expression of genes encoding Bcl-X_L, survivin, and Hsp70 remained elevated in *gp130*^{Y757F} compared to control mice (Figure 6B; data not shown). Compared to wild-type mice, we also noted in *gp130*^{Y757F} mice a more pronounced induction of *RegIIIb/Pap* mRNA (Figure 6B). Meanwhile, expression of RegIIIb/PAP protein and survivin was markedly decreased in *Stat3*$^{\Delta IEC}$ mice (Figures 7F and 7H), while epithelial cells comprising the CAC-dependent tumors in Stat3-proficient mice displayed strong expression of these proteins (Figures 7E and 7G). Collectively, these results strongly support the notion that the Stat3-associated antiapoptotic, prosurvival effects not only are present within preneoplastic cells during early tumor promotion in the CAC model but remain important for tumor epithelia.

DISCUSSION

A causal link between chronic inflammation and the development of cancer has long been recognized, and substantial insight into the underlying molecular mechanisms has been obtained in recent years. A large body of evidence suggests that Stat3, along with NF-κB, is one of the few key regulatory signaling molecules whose aberrant activation is invariably associated with inflammation and cancer, yet genetic evidence confirming such a role for Stat3 is still outstanding. With the advent of tissue-specific gene manipulation, it has become clear that Stat3 plays nonredundant roles in shaping the inflammatory response elicited by both proinflammatory stimuli belonging predominantly to the gp130 family of cytokines as well as anti-inflammatory signals elicited by IL-10-related cytokines. In turn, this balance has been postulated to modulate the tumor microenvironment, including the provision to subvert antitumor immune response. Meanwhile, emerging evidence suggests a central role for Stat3 in providing a transcriptional node for cancer cell-autonomous initiation of a tumor-promoting gene signature associated with proliferation, survival, and angiogenesis.

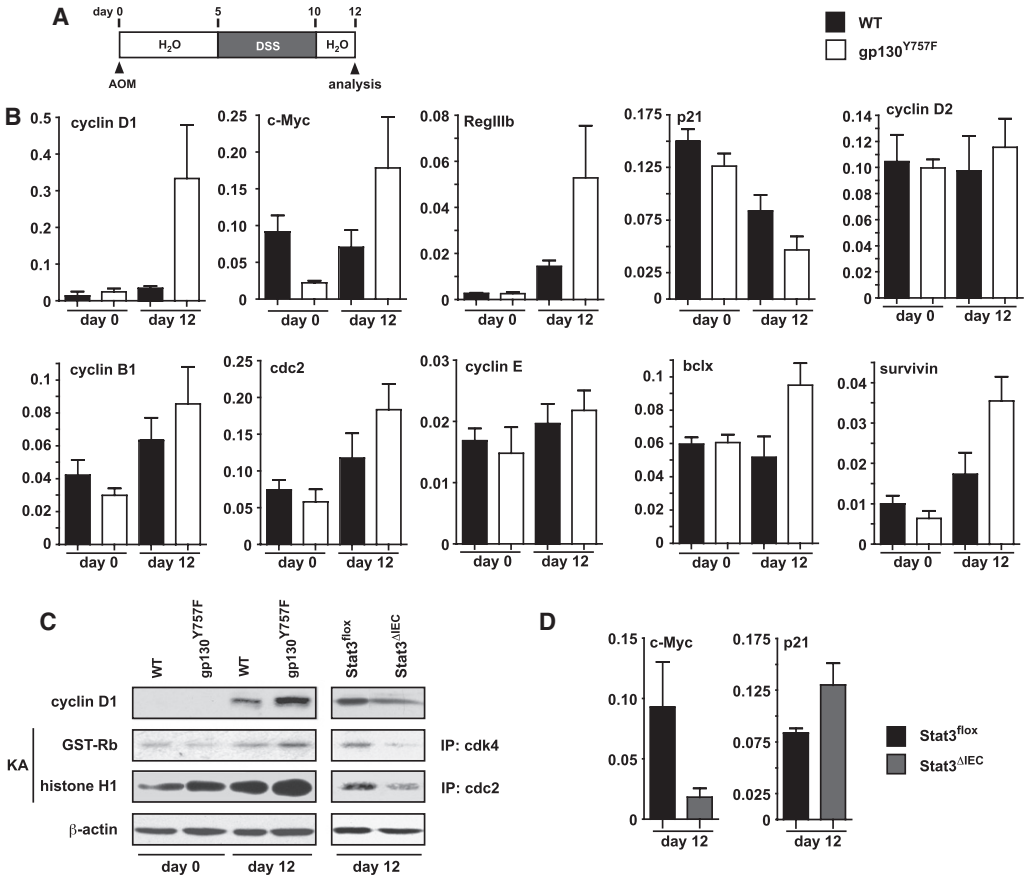

Figure 6. Stat3 Controls Expression of G1/S and G2/M Regulators

(A) Schematic representation of the initial steps of the CAC challenge that results in maximal proliferative response on day 12 of the CAC regimen.

(B) Expression of cell-cycle and apoptosis regulators in isolated intestinal epithelial cells (IECs) of wild-type (WT; black bars) and *gp130*^{Y757F} mice (white bars) before or at day 12 of the CAC challenge. Relative expression levels of mRNAs were determined by real-time PCR. Data are mean ± SEM.

(C) Immunoblot analysis of cyclin D1 and immunocomplex kinase assay of cdk4 and cdc2 prepared from isolated IECs of WT, *gp130*^{Y757F}, and *Stat3*$^{\Delta IEC}$ mice before or at day 12 of the CAC challenge.

(D) Relative expression levels of mRNAs encoding c-Myc and p21 in *Stat3*^{flox} (black bars) and *Stat3*$^{\Delta IEC}$ mice (gray bars) at day 12 of the CAC challenge. Data are mean ± SEM.

Although a number of growth factors as well as cell-intrinsic (epi)mutations have been associated with aberrant Stat3 activation during metaplastic transformation (Ernst et al., 2008; Miyatsuka et al., 2006) and in cancers of epithelial origin, the IL-6 family cytokines have recently been proposed to provide one of the missing links between inflammation and cancer (Naugler and Karin, 2008). Using a tissue-specific gain- and loss-of-function approach, we have provided direct genetic evidence that the gp130/Stat3 signaling axis indeed comprises a nonredundant regulatory component within the microenvironment of inflammation-associated tumors. Significantly, Stat3 stimulates both cell survival and proliferation (most likely alongside tumor angiogenesis), which explains the profound tumor-suppressive phenotype observed in *Stat3*$^{\Delta IEC}$ mice. This is in contrast to the role played by epithelial NF-κB in the CAC model, where we previously found that IEC-specific ablation of IKKβ profoundly suppresses tumor incidence without affecting tumor size (Greten et al., 2004). This phenotype results from excessive apoptosis during early tumor promotion, with an associated loss of mutagenized cells in which AOM induces the tumor-initiating insult. Indeed, suppression of the survival gene *bcl-x*, which is a molecular target for both NF-κB and Stat3, is a common observation during the early mucosal response to the DSS insult in lesions of *IKK*β$^{\Delta IEC}$ and *Stat3*$^{\Delta IEC}$ mice. Furthermore, this also coincides in *Stat3*$^{\Delta IEC}$ mice with impaired induction of survivin and Hsp70. In agreement, administration of IKKβ-specific inhibitors to wild-type mice during DSS-induced colitis is associated with reduced Stat3 activation and Hsp70 expression and impaired mucosal healing (Eckmann et al., 2008). In contrast to the observation presented here, where IEC-specific Stat3 ablation suppressed epithelial proliferation through a cell-autonomous mechanism in normal (i.e., in the acute DSS-induced colitis model) as well as in mutagenized mucosa (i.e., in the CAC model), such an effect was only observed following genetic blockage of NF-κB activation in myeloid cells of *IKK*β$^{\Delta mye}$ mice, but not in enterocytes of their *IKK*β$^{\Delta IEC}$ counterparts. We attributed these findings to the reduced production of paracrine-acting, tumor-promoting gp130 family cytokines by inflammation-associated, IKKβ-deficient macrophages and neutrophils. These observations together with the results presented here collectively provide

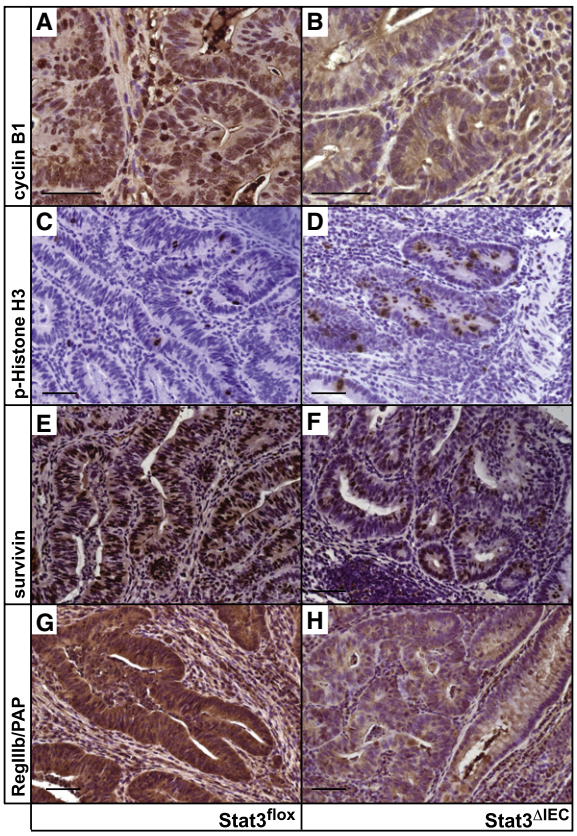

Figure 7. Loss of Stat3 Induces Mitotic Arrest in Preneoplastic Lesions

(A–H) Immunohistochemical analysis of cyclin B1 (A and B), phosphohistone H3 (C and D), survivin (E and F), and RegIIIb/PAP (G and H) in tumors from *Stat3*^{flox} mice (A, C, E, and G) and intraepithelial neoplasias found in *Stat3*$^{\Delta IEC}$ mice (B, D, F, and H) at the end of the CAC model on day 84. Scale bars = 100 μm.

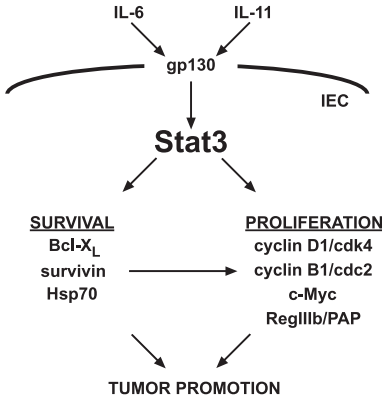

Figure 8. Schematic Overview of gp130/Stat3-Mediated Effects on Tumor Promotion

During CAC, both IL-6 and IL-11 induce gp130-mediated Stat3 activation. Stat3 comprises a central node responsible for cell survival and proliferation by regulating various downstream targets that ultimately favor accumulation and promotion of mutated cells.

evidence that myeloid NF-κB and IEC Stat3 provide the functional link by which inflammatory cells in the tumor microenvironment stimulate proliferation and promote tumor growth. Unlike the proposed function for NF-κB in myeloid cells, analogous Stat3 ablation in *Mx-Cre/Stat3*^{flox} (Alonzi et al., 2004) or *LysM-Cre/Stat3*^{flox} mice (Takeda et al., 1999) increased susceptibility to spontaneous colitis by virtue of disrupting the anti-inflammatory activity transduced by IL-10. In findings complementary to our observations here, elevated bacterial load in Il10-deficient mice frequently culminates in the development of colorectal cancer (Berg et al., 1996).

Our data support recent circumstantial evidence implicating the gp130/Stat3 signaling cascade in inflammation-associated cancer of the skin (Chan et al., 2004) and the gastrointestinal tract. We previously demonstrated that the initiation of spontaneously arising metaplastic gastric cancer in *gp130*^{Y757F} mice is refractory to antimicrobial treatment (Judd et al., 2006) and genetic reduction of Stat3 expression (Jenkins et al., 2005), while established lesions depend on continuous Stat3 activation (Ernst et al., 2008). Similarly, IEC-specific deletion of the negative feedback regulator Socs3 enables excessive Stat3 activation during the course of the CAC challenge and is associated with increased tumor numbers (Rigby et al., 2007). Meanwhile, in the same model, inhibition of IL-6-dependent *trans*-signaling reduces Stat3 phosphorylation and mucosal proliferation (Becker et al., 2004). Our results here extend these observations by providing functional evidence that, among the gp130-activating cytokines, at least IL-6- and IL-11-dependent Stat3 activation promotes CAC development by regulating the G1 and G2/M phases of the cell cycle. Thus, Stat3 activation provides one of the cell-autonomous mechanisms that functionally link inflammation-associated cytokines in the tumor microenvironment to the tumorigenic expansion of latent cancer cells.

Here we identify a number of aberrantly expressed effector proteins, some of which have been validated by other studies as bona fide Stat3 target genes and whose aberrant expression coincides with excessive phospho-Stat3 in various human cancers. It is therefore highly likely that, for instance, Hsp70, RegIIIb/PAP, survivin, cyclin B1, cdc2, c-Myc, and cyclin D1 are also intimately involved in mediating survival and proliferation of IECs in the CAC model (Figure 8). Indeed, Hsp70 is an important antiapoptotic factor for IECs (Sikora and Grzesiuk, 2007) and confers protection to colonic epithelia against DSS-induced damage (Tanaka et al., 2007). Furthermore, IFN-γ and IL-6 induce expression of the C-type lectin RegIIIb/PAP, which is upregulated in DSS-induced colitis in mice as well as in human inflammatory bowel disease (te Velde et al., 2007) and in 60% of colon cancers (Macadam et al., 2000). Significantly, Stat3-mediated signaling in response to the IL-10 family cytokine IL-22 protects against experimental colitis (Sugimoto et al., 2008). This observation correlates with enhanced expression of RegIIIb/PAP along with several mucins (Zheng et al., 2008), which are also upregulated in untreated *gp130*^{Y757F} mice (data not shown). The bifunctional role of the small inhibitor of apoptosis (IAP) family protein survivin in counteracting apoptosis as well as controlling mitogenic progression (Altieri, 2008) is likely to provide a functional explanation for some of our observations on cell-cycle protein expression. In untransformed cells, survivin is selectively expressed during the G2/M transition, localizes to mitotic spindle microtubules (Li et al., 1998), and is phosphorylated by physical association with cdc2 (O'Connor et al., 2000), while siRNA-mediated

survivin knockdown induces a G2/M arrest in human colorectal cancer cells (Rodel et al., 2005). In preneoplastic lesions of *Stat3*$^{\Delta IEC}$ mice, impaired survivin expression may also account for the increase in phosphohistone H3-positive cells indicating a mitotic arrest. Finally, cucurbitacin I-mediated inhibition of Stat3 (Blaskovich et al., 2003) induces cell-cycle arrest at the G2/M transition in cell lines derived from either laryngeal squamous cell carcinoma or glioblastoma multiforme, which, similar to our observations in lesions from *Stat3*$^{\Delta IEC}$ mice, is associated with the downregulation of cyclin B1 and cdc2 (Liu et al., 2008; Su et al., 2008). However, it remains to be established whether Stat3 can regulate cyclin B1 in IECs directly, as recently suggested in other cell types (Snyder et al., 2008).

The high prevalence of activating *Catnb* mutations in AOM-induced tubular adenomas irrespective of the compounding mutations in the gp130/Stat3 signaling cascade observed here suggests a putative role for Stat3 in executing a strong modifier function for colorectal tumors carrying activating mutations in the canonical Wnt pathway. This function requires the supply of gp130 family ligands from infiltrating inflammatory cells, which promote intestinal polyposis in the *Apc*^{Min} mouse model (Rakoff-Nahoum and Medzhitov, 2007) where aberrant Wnt signaling results from stochastic loss-of-heterozygosity mutations of the tumor suppressor gene *Apc* in the epithelial stem cell compartment. Thus, tumor load is reduced in *Apc*^{Min}/*Il6*$^{-/-}$ compound mutant mice (Baltgalvis et al., 2008), while their *Apc*^{Min}/*gp130*^{Y757F} counterparts show increased tumor multiplicity (T.J.P. and M.E., unpublished data). Although the exact mechanism remains to be elucidated, it is conceivable that the canonical Wnt and Stat3 pathways intersect on common molecular targets including c-*myc* and *cyclin D1* to induce transcription above the threshold required for cell-cycle progression. On the other hand, the failure to eliminate cyclin D1 due to sustained Stat3 activation may bypass the DNA replication checkpoint response (Shields et al., 2008), which is likely to impact aberrant chromosome segregation triggered in the absence of functional Apc protein (Dikovskaya et al., 2007).

Several compounds targeting Stat3 have shown promising results in cultured cells and preclinical models (Darnell, 2005; Groner et al., 2008). Although excessive interference with systemic Stat3 activation is likely to curtail the beneficial anti-inflammatory response of macrophages, with the potential consequence of further fueling gastrointestinal inflammation, Stat3-dependent cancers are generally highly sensitive to small reductions in Stat3 activity. The resulting therapeutic window may therefore allow systemic delivery of Stat3 inhibitors to indirectly "target" Stat3-addicted tumors with beneficial selectivity (Ernst et al., 2008) while still enhancing T cell-mediated antitumor activities (Yu et al., 2007). In the context of inflammation-associated gastrointestinal cancers, the validity and efficacy of such strategies need to be assessed against, or in combination with, inhibitors of the myeloid NF-κB/IL-6 signaling axis as well as those directed against IL-11.

EXPERIMENTAL PROCEDURES

Mice and CAC Model

To delete *Stat3* in IECs, we crossed *Stat3*$^{lox/lox}$ mice (termed *Stat3*^{flox}) (Takeda et al., 1998) to *villin*-Cre transgenic mice (Madison et al., 2002), which were backcrossed for four generations on an FVB background before intercrossing to generate compound mutant *villin*-Cre/*Stat3*$^{lox/lox}$ mice (termed *Stat3*$^{\Delta IEC}$). Mutant *gp130*$^{Y757F/Y757F}$ mice (termed *gp130*^{Y757F}), as well as their compound derivatives *gp130*^{Y757F}/*Il6*$^{-/-}$, *gp130*^{Y757F}/*Il11ra*$^{-/-}$, *gp130*^{Y757F}/*Stat3*$^{+/-}$, and *gp130*^{Y757F}/*Stat1*$^{+/-}$ mice, were all on a C57BL/6 × 129Sv background and have been described previously (Ernst et al., 2008). The CAC model was performed essentially as described previously (Greten et al., 2004) using 10 mg/kg azoxymethane (AOM; Sigma-Aldrich) and 3.5% dextran sulfate sodium (DSS; MP Biomedicals). Histological assessment of colitis was performed as described previously (Eckmann et al., 2008; Greten et al., 2004). In all experiments, littermate controls were used to assure comparison of mice on the same genetic background. All procedures were approved by the Ludwig Institute for Cancer Research, Department of Surgery Committee and the Regierung von Oberbayern, respectively.

Determination of Proliferation, Migration Rates, and Apoptosis

Mice were injected intraperitoneally with 100 mg/kg BrdU (Sigma) 1.5 hr prior to sacrifice, and paraffin sections were stained using anti-BrdU antibody (Amersham Biosciences RPN201). For determination of migration rates, BrdU-injected mice were sacrificed 48 hr after injection. For each analysis, BrdU-positive cells were scored in 12 full crypts from three animals of each genotype. Apoptosis was determined by TUNEL assay using an ApoAlert DNA Fragmentation Assay Kit (BD Clontech).

Protein Analysis and Immunohistochemistry

Isolation of enterocytes, immunoblot analysis, and immunocomplex kinase assay were essentially performed as described previously (Greten et al., 2004). Paraffin sections (3.5 μm) were stained using standard immunohistochemical procedures. Antibodies used were anti-Stat3 (SC-482), anti-Stat1 (SC-346, Santa Cruz), anti-phospho-Stat3 (9145), anti-cleaved caspase-3 (9661), anti-caspase-9 (9504), anti-survivin (2808), anti-phosphohistone H3 (9701, Cell Signaling), anti-HSP70 (SPA-810, Stressgen), anti-Bcl-2 (610539), anti-Bcl-X_L (556499), anti-Bax (554106, BD Pharmingen), anti-β-catenin (UBI 6734), anti-RegIIIb/PAP (Algul et al., 2007), anti-Mcl-1 (SC-819), anti-Bak (SC-832), anti-Fas (SC-1024), anti-cyclin D1 (SC-718), anti-c-Myc (SC-788), anti-cyclin B1 (SC-752, Santa Cruz), and anti-β-actin (A4700, Sigma).

RNA Analysis

Total RNA was extracted from isolated enterocytes using an RNeasy Mini Kit (QIAGEN). SuperScript II Reverse Transcriptase (Invitrogen) was used for synthesis of cDNA. Real-time PCR analysis using Power SYBR Green PCR Master Mix (Applied Biosystems) was performed on a StepOne Plus Real-Time PCR System (Applied Biosystems). Primer sequences are listed in Supplemental Experimental Procedures.

Statistical Analysis

Data are expressed as mean ± SEM. Differences were analyzed by one-way ANOVA or Student's t test. $p \leq 0.05$ was considered significant.

SUPPLEMENTAL DATA

The Supplemental Data include Supplemental Experimental Procedures and six figures and can be found with this article online at http://www.cancercell.org/supplemental/S1535-6108(09)00003-8.

ACKNOWLEDGMENTS

We thank B. Wittig, K. Retzlaff, and V. Feakes for excellent technical assistance. We also thank D. Gumucio for providing *villin*-Cre mice and W. Reindl for providing *Stat3*$^{lox/lox}$ mice with the permission of K. Takeda. M.C.A. was supported by grants obtained from the Wilhelm Sander-Stiftung (2005.146.1) and Deutsche Krebshilfe (107977). M.E. was supported by the National Health and Medical Research Council of Australia (NHMRC) and by an NHMRC Senior Research Fellowship. F.R.G. was supported by the Deutsche Forschungsgemeinschaft (Emmy Noether Programme Gr1916/2-2, SFB 456), Deutsche Krebshilfe (106772), and Fritz Thyssen Stiftung (10.05.2.168).

Received: August 22, 2008
Revised: November 9, 2008
Accepted: January 6, 2009
Published: February 2, 2009

REFERENCES

Algul, H., Treiber, M., Lesina, M., Nakhai, H., Saur, D., Geisler, F., Pfeifer, A., Paxian, S., and Schmid, R.M. (2007). Pancreas-specific RelA/p65 truncation increases susceptibility of acini to inflammation-associated cell death following cerulein pancreatitis. J. Clin. Invest. *117*, 1490–1501.

Alonzi, T., Newton, I.P., Bryce, P.J., Di Carlo, E., Lattanzio, G., Tripodi, M., Musiani, P., and Poli, V. (2004). Induced somatic inactivation of STAT3 in mice triggers the development of a fulminant form of enterocolitis. Cytokine *26*, 45–56.

Altieri, D.C. (2008). Survivin, cancer networks and pathway-directed drug discovery. Nat. Rev. Cancer *8*, 61–70.

Ancrile, B., Lim, K.H., and Counter, C.M. (2007). Oncogenic Ras-induced secretion of IL6 is required for tumorigenesis. Genes Dev. *21*, 1714–1719.

Baltgalvis, K.A., Berger, F.G., Pena, M.M., Davis, J.M., Muga, S.J., and Carson, J.A. (2008). Interleukin-6 and cachexia in ApcMin/+ mice. Am. J. Physiol. Regul. Integr. Comp. Physiol. *294*, R393–R401.

Becker, C., Fantini, M.C., Schramm, C., Lehr, H.A., Wirtz, S., Nikolaev, A., Burg, J., Strand, S., Kiesslich, R., Huber, S., et al. (2004). TGF-beta suppresses tumor progression in colon cancer by inhibition of IL-6 trans-signaling. Immunity *21*, 491–501.

Berg, D.J., Davidson, N., Kuhn, R., Muller, W., Menon, S., Holland, G., Thompson-Snipes, L., Leach, M.W., and Rennick, D. (1996). Enterocolitis and colon cancer in interleukin-10-deficient mice are associated with aberrant cytokine production and CD4(+) TH1-like responses. J. Clin. Invest. *98*, 1010–1020.

Blaskovich, M.A., Sun, J., Cantor, A., Turkson, J., Jove, R., and Sebti, S.M. (2003). Discovery of JSI-124 (cucurbitacin I), a selective Janus kinase/signal transducer and activator of transcription 3 signaling pathway inhibitor with potent antitumor activity against human and murine cancer cells in mice. Cancer Res. *63*, 1270–1279.

Catlett-Falcone, R., Landowski, T.H., Oshiro, M.M., Turkson, J., Levitzki, A., Savino, R., Ciliberto, G., Moscinski, L., Fernandez-Luna, J.L., Nunez, G., et al. (1999). Constitutive activation of Stat3 signaling confers resistance to apoptosis in human U266 myeloma cells. Immunity *10*, 105–115.

Chan, K.S., Sano, S., Kiguchi, K., Anders, J., Komazawa, N., Takeda, J., and DiGiovanni, J. (2004). Disruption of Stat3 reveals a critical role in both the initiation and the promotion stages of epithelial carcinogenesis. J. Clin. Invest. *114*, 720–728.

Darnell, J.E. (2005). Validating Stat3 in cancer therapy. Nat. Med. *11*, 595–596.

Dikovskaya, D., Schiffmann, D., Newton, I.P., Oakley, A., Kroboth, K., Sansom, O., Jamieson, T.J., Meniel, V., Clarke, A., and Nathke, I.S. (2007). Loss of APC induces polyploidy as a result of a combination of defects in mitosis and apoptosis. J. Cell Biol. *176*, 183–195.

Eckmann, L., Nebelsiek, T., Fingerle, A.A., Dann, S.M., Mages, J., Lang, R., Robine, S., Kagnoff, M.F., Schmid, R.M., Karin, M., et al. (2008). Opposing functions of IKKbeta during acute and chronic intestinal inflammation. Proc. Natl. Acad. Sci. USA *105*, 15058–15063.

El Kasmi, K.C., Holst, J., Coffre, M., Mielke, L., de Pauw, A., Lhocine, N., Smith, A.M., Rutschman, R., Kaushal, D., Shen, Y., et al. (2006). General nature of the STAT3-activated anti-inflammatory response. J. Immunol. *177*, 7880–7888.

Ernst, M., Najdovska, M., Grail, D., Lundgren-May, T., Buchert, M., Tye, H., Matthews, V.B., Armes, J., Bhathal, P.S., Hughes, N.R., et al. (2008). STAT3 and STAT1 mediate IL-11-dependent and inflammation-associated gastric tumorigenesis in gp130 receptor mutant mice. J. Clin. Invest. *118*, 1727–1738.

Gao, S.P., Mark, K.G., Leslie, K., Pao, W., Motoi, N., Gerald, W.L., Travis, W.D., Bornmann, W., Veach, D., Clarkson, B., et al. (2007). Mutations in the EGFR kinase domain mediate STAT3 activation via IL-6 production in human lung adenocarcinomas. J. Clin. Invest. *117*, 3846–3856.

Greten, F.R., Eckmann, L., Greten, T.F., Park, J.M., Li, Z.W., Egan, L.J., Kagnoff, M.F., and Karin, M. (2004). IKKbeta links inflammation and tumorigenesis in a mouse model of colitis-associated cancer. Cell *118*, 285–296.

Grivennikov, S., Karin, E., Terzic, J., Mucida, D., Yu, G.-Y., Vallabhapurapu, S., Scheller, J., Rose-John, S., Cheroutre, H., Eckmann, L., and Karin, M. (2009). IL-6 and Stat3 are required for survival of intestinal epithelial cells and development of colitis-associated cancer. Cancer Cell *15*, this issue, 103–113.

Groner, B., Lucks, P., and Borghouts, C. (2008). The function of Stat3 in tumor cells and their microenvironment. Semin. Cell Dev. Biol. *19*, 341–350.

Hanahan, D., and Weinberg, R.A. (2000). The hallmarks of cancer. Cell *100*, 57–70.

He, B., You, L., Uematsu, K., Zang, K., Xu, Z., Lee, A.Y., Costello, J.F., McCormick, F., and Jablons, D.M. (2003). SOCS-3 is frequently silenced by hypermethylation and suppresses cell growth in human lung cancer. Proc. Natl. Acad. Sci. USA *100*, 14133–14138.

Heinrich, P.C., Behrmann, I., Haan, S., Hermanns, H.M., Muller-Newen, G., and Schaper, F. (2003). Principles of interleukin (IL)-6-type cytokine signalling and its regulation. Biochem. J. *374*, 1–20.

Jenkins, B.J., Grail, D., Nheu, T., Najdovska, M., Wang, B., Waring, P., Inglese, M., McLoughlin, R.M., Jones, S.A., Topley, N., et al. (2005). Hyperactivation of Stat3 in gp130 mutant mice promotes gastric hyperproliferation and desensitizes TGF-beta signaling. Nat. Med. *11*, 845–852.

Judd, L.M., Bredin, K., Kalantzis, A., Jenkins, B.J., Ernst, M., and Giraud, A.S. (2006). STAT3 activation regulates growth, inflammation, and vascularization in a mouse model of gastric tumorigenesis. Gastroenterology *131*, 1073–1085.

Karin, M., and Greten, F.R. (2005). NF-kappaB: linking inflammation and immunity to cancer development and progression. Nat. Rev. Immunol. *5*, 749–759.

Levy, D.E., and Darnell, J.E., Jr. (2002). Stats: transcriptional control and biological impact. Nat. Rev. Mol. Cell Biol. *3*, 651–662.

Li, F., Ambrosini, G., Chu, E.Y., Plescia, J., Tognin, S., Marchisio, P.C., and Altieri, D.C. (1998). Control of apoptosis and mitotic spindle checkpoint by survivin. Nature *396*, 580–584.

Liu, T., Zhang, M., Zhang, H., Sun, C., and Deng, Y. (2008). Inhibitory effects of cucurbitacin B on laryngeal squamous cell carcinoma. Eur. Arch. Otorhinolaryngol. *265*, 1225–1232.

Macadam, R.C., Sarela, A.I., Farmery, S.M., Robinson, P.A., Markham, A.F., and Guillou, P.J. (2000). Death from early colorectal cancer is predicted by the presence of transcripts of the REG gene family. Br. J. Cancer *83*, 188–195.

Madison, B.B., Dunbar, L., Qiao, X.T., Braunstein, K., Braunstein, E., and Gumucio, D.L. (2002). Cis elements of the villin gene control expression in restricted domains of the vertical (crypt) and horizontal (duodenum, cecum) axes of the intestine. J. Biol. Chem. *277*, 33275–33283.

Mantovani, A., Allavena, P., Sica, A., and Balkwill, F. (2008). Cancer-related inflammation. Nature *454*, 436–444.

Miyatsuka, T., Kaneto, H., Shiraiwa, T., Matsuoka, T.A., Yamamoto, K., Kato, K., Nakamura, Y., Akira, S., Takeda, K., Kajimoto, Y., et al. (2006). Persistent expression of PDX-1 in the pancreas causes acinar-to-ductal metaplasia through Stat3 activation. Genes Dev. *20*, 1435–1440.

Naugler, W.E., and Karin, M. (2008). The wolf in sheep's clothing: the role of interleukin-6 in immunity, inflammation and cancer. Trends Mol. Med. *14*, 109–119.

O'Connor, D.S., Grossman, D., Plescia, J., Li, F., Zhang, H., Villa, A., Tognin, S., Marchisio, P.C., and Altieri, D.C. (2000). Regulation of apoptosis at cell division by p34cdc2 phosphorylation of survivin. Proc. Natl. Acad. Sci. USA *97*, 13103–13107.

Rakoff-Nahoum, S., and Medzhitov, R. (2007). Regulation of spontaneous intestinal tumorigenesis through the adaptor protein MyD88. Science *317*, 124–127.

Rigby, R.J., Simmons, J.G., Greenhalgh, C.J., Alexander, W.S., and Lund, P.K. (2007). Suppressor of cytokine signaling 3 (SOCS3) limits damage-induced crypt hyper-proliferation and inflammation-associated tumorigenesis in the colon. Oncogene *26*, 4833–4841.

Rodel, F., Hoffmann, J., Distel, L., Herrmann, M., Noisternig, T., Papadopoulos, T., Sauer, R., and Rodel, C. (2005). Survivin as a radioresistance factor, and prognostic and therapeutic target for radiotherapy in rectal cancer. Cancer Res. *65*, 4881–4887.

Shields, B.J., Hauser, C., Bukczynska, P.E., Court, N.W., and Tiganis, T. (2008). DNA replication stalling attenuates tyrosine kinase signaling to suppress S phase progression. Cancer Cell *14*, 166–179.

Sikora, A., and Grzesiuk, E. (2007). Heat shock response in gastrointestinal tract. J. Physiol. Pharmacol. *58*(*Suppl 3*), 43–62.

Snyder, M., Huang, X.Y., and Zhang, J.J. (2008). Identification of novel direct Stat3 target genes for control of growth and differentiation. J. Biol. Chem. *283*, 3791–3798.

Stuhlmann-Laeisz, C., Lang, S., Chalaris, A., Krzysztof, P., Enge, S., Eichler, J., Klingmuller, U., Samuel, M., Ernst, M., Rose-John, S., et al. (2006). Forced dimerization of gp130 leads to constitutive STAT3 activation, cytokine-independent growth, and blockade of differentiation of embryonic stem cells. Mol. Biol. Cell *17*, 2986–2995.

Su, Y., Li, G., Zhang, X., Gu, J., Zhang, C., Tian, Z., and Zhang, J. (2008). JSI-124 inhibits glioblastoma multiforme cell proliferation through G(2)/M cell cycle arrest and apoptosis augment. Cancer Biol. Ther. *7*, 1243–1249.

Sugimoto, K., Ogawa, A., Mizoguchi, E., Shimomura, Y., Andoh, A., Bhan, A.K., Blumberg, R.S., Xavier, R.J., and Mizoguchi, A. (2008). IL-22 ameliorates intestinal inflammation in a mouse model of ulcerative colitis. J. Clin. Invest. *118*, 534–544.

Takeda, K., Kaisho, T., Yoshida, N., Takeda, J., Kishimoto, T., and Akira, S. (1998). Stat3 activation is responsible for IL-6-dependent T cell proliferation through preventing apoptosis: generation and characterization of T cell-specific Stat3-deficient mice. J. Immunol. *161*, 4652–4660.

Takeda, K., Clausen, B.E., Kaisho, T., Tsujimura, T., Terada, N., Forster, I., and Akira, S. (1999). Enhanced Th1 activity and development of chronic enterocolitis in mice devoid of Stat3 in macrophages and neutrophils. Immunity *10*, 39–49.

Tanaka, K., Namba, T., Arai, Y., Fujimoto, M., Adachi, H., Sobue, G., Takeuchi, K., Nakai, A., and Mizushima, T. (2007). Genetic evidence for a protective role for heat shock factor 1 and heat shock protein 70 against colitis. J. Biol. Chem. *282*, 23240–23252.

Tebbutt, N.C., Giraud, A.S., Inglese, M., Jenkins, B., Waring, P., Clay, F.J., Malki, S., Alderman, B.M., Grail, D., Hollande, F., et al. (2002). Reciprocal regulation of gastrointestinal homeostasis by SHP2 and STAT-mediated trefoil gene activation in gp130 mutant mice. Nat. Med. *8*, 1089–1097.

te Velde, A.A., de Kort, F., Sterrenburg, E., Pronk, I., ten Kate, F.J., Hommes, D.W., and van Deventer, S.J. (2007). Comparative analysis of colonic gene expression of three experimental colitis models mimicking inflammatory bowel disease. Inflamm. Bowel Dis. *13*, 325–330.

Yu, H., and Jove, R. (2004). The STATs of cancer–new molecular targets come of age. Nat. Rev. Cancer *4*, 97–105.

Yu, H., Kortylewski, M., and Pardoll, D. (2007). Crosstalk between cancer and immune cells: role of STAT3 in the tumour microenvironment. Nat. Rev. Immunol. *7*, 41–51.

Zhang, X., Guo, A., Yu, J., Possemato, A., Chen, Y., Zheng, W., Polakiewicz, R.D., Kinzler, K.W., Vogelstein, B., Velculescu, V.E., et al. (2007). Identification of STAT3 as a substrate of receptor protein tyrosine phosphatase T. Proc. Natl. Acad. Sci. USA *104*, 4060–4064.

Zheng, Y., Valdez, P.A., Danilenko, D.M., Hu, Y., Sa, S.M., Gong, Q., Abbas, A.R., Modrusan, Z., Ghilardi, N., de Sauvage, F.J., et al. (2008). Interleukin-22 mediates early host defense against attaching and effacing bacterial pathogens. Nat. Med. *14*, 282–289.